

Intercomparison and evaluation of atmospheric transport in a Lagrangian model (STOCHEM), and an Eulerian model (UM), using ^{222}Rn as a short-lived tracer.

By D. S. STEVENSON*, W. J. COLLINS, C. E. JOHNSON and R. G. DERWENT
Meteorological Office, UK

(Received 20 January 1997; revised 5 December 1997)

SUMMARY

Transport of the short-lived (half-life 3.83 days) isotope ^{222}Rn , which is emitted from unfrozen soils, is used to compare transport in several versions of the UK Meteorological Office Lagrangian chemistry-transport model and in the Unified Model, the UK Meteorological Office general circulation model. The same ^{222}Rn experiment is repeated for all the model versions, illustrating the impact on global transport of various model improvements: adding boundary-layer schemes, including sub-grid scale convection, increasing model spatial resolution, and increasing the temporal resolution of the meteorological fields used for driving the off-line model. Results from all model versions are compared with a limited observational data set, and also with results from the same ^{222}Rn simulations carried out with several global atmospheric transport models as part of the World Climate Research Program in December 1993 (Jacob *et al.* 1997). Versions of the Lagrangian chemistry-transport model that include sub-grid scale convection, transport ^{222}Rn in a manner that is similar to the Unified Model and most general circulation models, supporting the simple and computationally inexpensive Lagrangian approach taken.

KEYWORDS: Eulerian model Lagrangian model ^{222}Rn 3-D model Transport

1. INTRODUCTION

The UK Meteorological Office (UKMO) chemistry-transport model (STOCHEM) uses a Lagrangian transport scheme, where currently 10 000–50 000 equal mass air parcels are advected using 3-D wind fields from the UK Meteorological Office Unified Model (UM). The UM is an Eulerian general circulation model (GCM) and can be operated at several resolutions, two of which will be discussed here: (i) climate resolution, 3.75° (longitude) \times 2.5° (latitude) \times 19 vertical levels; and (ii) operational resolution, 1.25° \times 0.833° \times 19 vertical levels. In this paper, tracer transport within several versions of STOCHEM is compared by performing simulations of the atmospheric distribution of the short-lived radio-isotope ^{222}Rn , which is emitted from unfrozen soils. The comparisons illustrate the impact of adding new features to this model: a parametrized boundary layer, a sub-grid scale convection scheme, and increasing the temporal and spatial resolution.

A direct comparison between the tracer transport schemes of STOCHEM and the UM is also included, where meteorological fields output from a UM tracer experiment at climate resolution are used to drive exactly the same experiment using STOCHEM. This comparison was used to tune the sub-grid scale convection parametrization in STOCHEM; this scheme causes rapid vertical mixing in areas of convective cloud. ^{222}Rn results are also compared to observations and to a wider model intercomparison carried out by Jacob *et al.* (1997), under the auspices of the World Climate Research Program (WCRP), which included most of the major GCMs currently in use throughout the world.

STOCHEM is usually used with 50–70 chemical species, which are subject to chemical and photochemical reactions and physical processes such as dry and wet deposition, as well as transport (e.g. Collins *et al.* 1997; Stevenson *et al.* 1997). Within an Eulerian framework, this would require the solution of the advection–diffusion equation for each individual species, which would be computationally expensive. Within the Lagrangian framework, transport and diffusion are decoupled from the chemistry, by transporting individual air parcels with a three-hour time-step, calculating the chemical evolution of each air parcel with a five-minute time-step, then applying some inter-parcel mixing between

* Corresponding author: Atmospheric Processes Research, Meteorological Office, London Road, Bracknell, RG12 2SZ, UK.

TABLE 1. SUMMARY OF MODEL VERSIONS (SEE SECTION 3 FOR FULL DETAILS).

Version	No. parcels	Met. data res. ¹	Output res. ²	BL	<i>D</i>	Convection
a	10 000	0.83 × 1.25 × 9 × 18d	10 × 10 × 9	1 layer	0.3	N
b	10 000	0.83 × 1.25 × 9 × 18d	10 × 10 × 9	UM	0.3	N
c	10 000	0.83 × 1.25 × 9 × 18d	10 × 10 × 9	UM+NAME	10 ⁻³ /10 ⁻⁶	N
d	10 000	0.83 × 1.25 × 9 × 18d	10 × 10 × 9	UM+NAME	10 ⁻³ /10 ⁻⁶	Y†
e	10 000	0.83 × 1.25 × 9 × 18d	10 × 10 × 9	UM+NAME	10 ⁻³ /10 ⁻⁶	Y
5×5o	50 000	0.83 × 1.25 × 9 × 18d	5 × 5 × 9	UM+NAME	10 ⁻³ /10 ⁻⁶	Y
5×5c	50 000	2.5 × 3.75 × 19 × 6h	5 × 5 × 10	UM+NAME	10 ⁻³ /10 ⁻⁶	Y
UM	Eulerian	2.5 × 3.75 × 19 × 0.5h	2.5 × 3.75 × 19	UM	—	UM

¹ Meteorological data resolution: latitude by longitude by number of vertical levels by time-step.

² Output resolution: latitude by longitude by number of vertical levels.

† Untuned convection.

advection steps. In this way, increasing the number of chemical species incurs no expense in terms of transport, only in terms of the chemistry computation. Hence a Lagrangian transport scheme has been employed within STOCHEM: here we compare the scheme to the transport within a tried and tested GCM, in order to evaluate its performance.

2. DESCRIPTION OF THE ²²²Rn EXPERIMENT

Essentially the same experiment was repeated for eight different model configurations (Table 1). Radon emissions were specified in the same way as at the WCRP workshop of August 1995. These emissions fields vary slightly, but not significantly, from those used at the WCRP workshop in December 1993 (Jacob *et al.* 1997). The radon source distribution was specified as: all land surfaces except Greenland and Antarctica, but no emissions south of 60°S or north of 70°N. The radon source strength was specified as: 0.5 atom cm⁻² s⁻¹ between 60°N and 70°N, and about 1 atom cm⁻² s⁻¹ between 60°N and 60°S, such that the global source strength is 15 kg yr⁻¹.

²²²Rn decays with a half-life of 3.83 days to ²¹⁰Pb, which attaches itself to pre-existing aerosol particles and is subsequently removed by rain-out processes. This daughter product can be used to investigate model precipitation scavenging, but it is not considered in the experiments described here. No other source or sink processes operate.

For participation in the WCRP 1993 workshop, standard experiment run lengths of 15 months were specified, with the first three months used as spin-up time. In this paper, only the UM results are from a run of this length. The versions of STOCHEM using operational model 18-day mean winds were run from the beginning of May to the end of August, with the first month as spin-up, whilst the version of STOCHEM using climate resolution six-hourly winds was run from the middle of June to the end of July, with the first two weeks as spin-up. Because of the short half-life of ²²²Rn, equilibrium global distributions are reached within about two weeks, so all of these runs can be considered to have reached equilibrium, and hence are comparable.

3. MODEL VERSIONS

(a) General description of STOCHEM

STOCHEM uses a Lagrangian transport scheme based upon the models of Walton *et al.* (1988) and Taylor (1989), and a similar approach has been taken in other global tropospheric chemistry models (Penner *et al.* 1991; Atherton *et al.* 1996). The lower

atmosphere (pressures above 100 hPa) is divided into 10 000 or 50 000 equal mass air parcels. The centroids of these air parcels are advected with a three-hour time-step using 3-D winds from the UM; acceleration terms are ignored. Two different advection schemes are used here, depending upon the spatial and temporal resolution of the meteorological data (see below).

A hybrid vertical coordinate (η) is used in all of the models, and is defined as follows:

$$\eta = P/P_s + A(1/P_0 - 1/P_s) \quad (1)$$

where P is pressure, P_s is surface pressure, P_0 is a reference pressure (1000 hPa), and A is a coefficient having the dimensions of pressure. A is set to zero near the surface and is equal to the pressure for pressures lower than 30 hPa. Hence near the surface η is terrain following and is equal to P/P_s , whilst above 30 hPa, η follows pressure surfaces and is equal to P/P_0 .

Each air parcel holds a ^{222}Rn concentration, initially set to zero. Air parcel concentrations are mapped onto an Eulerian grid for the purposes of inter-parcel mixing and output of results. The horizontal resolution of the Eulerian grid is also used for the surface ^{222}Rn emission field. After each advection time-step the emissions for a grid square are distributed equally over all the air parcels that are within the boundary layer above that grid square. If there are no air parcels within the boundary layer for a particular emissions grid square, then those emissions are stored until an air parcel does arrive. For model versions with 10 000 air parcels, an Eulerian grid resolution of 10° longitude by 10° latitude with nine vertical levels of thickness $\Delta\eta = 0.1$ (c.100 hPa) gives a typical grid occupancy of two air parcels. Model versions with 50 000 air parcels have a higher horizontal Eulerian grid resolution of 5° , but retain the same vertical resolution.

During advection, air parcels are considered to be isolated. In reality, there will be mixing with other air parcels by diffusion processes characteristic of the parcel size. The mixing ratio of a species in an air parcel (C), is brought closer to the average mixing ratio of the occupied Eulerian grid box (\bar{C}), by adding a term $D \cdot (\bar{C} - C)$, where D is a factor representing the degree of mixing. This factor varies in different model versions below.

(b) Meteorological data used to drive STOCHEM

Six of the runs described here used 18-day mean plus standard deviation meteorological fields (see Table 1), and this has been the main configuration used during the development stage of STOCHEM (e.g. Collins *et al.* 1995, 1997; Stevenson *et al.* 1995, 1997).

Mean fields were used for ease of data storage and manipulation. Fields were taken from the operational version of the UM, so have a high spatial resolution. Nine of the 19 vertical levels available are used for three-dimensional interpolations. Mean and standard deviations were calculated for cloud and boundary-layer parameters at four times of day: 0000, 0600, 1200 and 1800; wind, temperature, and pressure fields were averaged over all times. No meteorological significance is attached to the averaging period of 18 days; this was simply chosen for data processing reasons. Seven different 18-day mean data-sets were used for the four month runs described here, with a simple switch to the next data-set after each 18-day period.

Mean and standard deviation wind vectors for a particular Lagrangian air parcel are calculated from the cell position using a three-dimensional tri-linear interpolation. Wind components are then determined using the mean and a random fraction of the standard deviation:

$$v_i = \bar{v}_i + S_i\sigma_i + \frac{1}{2}\nabla_i\sigma_i^2; \quad i = x, y \text{ or } \eta \quad (2)$$

where \bar{v}_i is the mean wind component, σ_i is the standard deviation of the wind component, S_i is a normally-distributed random number and ∇_i is the i component of the gradient operator. The last term is a drift correction which takes into account the effect that the cell will tend to drift in the direction of increasing variance (Thomson 1987). Without this term, air parcels tend to accumulate in areas of low variance. The vertical velocity (v_η) is equivalent to $d\eta/dt$, and has units [s^{-1}].

Versions (a–e) have an Eulerian grid resolution of $10^\circ \times 10^\circ \times 9$ vertical levels, and used 10 000 Lagrangian air parcels. Horizontal resolution increases with the sixth version ($5 \times 5_o$), which used 50 000 air parcels.

The seventh model version ($5 \times 5_c$) also uses the higher horizontal resolution for mapping and mixing air parcels, and also adds a tenth vertical level to the Eulerian grid, between $\eta = 0.1$ – 0.01 . Meteorological data fields are from a climate resolution run of the UM, and are changed every six hours. Interpolated winds use all 19 vertical levels available from the climate run. To represent sub-grid scale components, random horizontal and vertical terms are added to winds (Maryon *et al.* 1991):

$$v_i = v_{\text{interpolated}} + S_i(2K_i/\Delta t)^{0.5}; \quad i = x, y \text{ or } \eta \quad (3)$$

where Δt is the advection time-step (three hours), K_x and K_y are horizontal diffusion coefficients ($5300 \text{ m}^2\text{s}^{-1}$ in the boundary layer, $1325 \text{ m}^2\text{s}^{-1}$ above the boundary layer), and K_η is the vertical diffusion coefficient (in η coordinates, $7 \times 10^{-9} \text{ s}^{-1}$).

(c) Boundary-layer treatment

Model version (a) includes the most basic boundary-layer scheme: emissions are simply added to air parcels in the lowermost Eulerian layer ($\eta = 1.0$ – 0.9). This is improved in version (b), where BL depths from the UM at four times of day are used; these are also specified as 18-day means with standard deviations. All the other versions of STOCHEM use the NAME model (Maryon *et al.* 1991) parametrization for vertical mixing within the BL and entrainment from the BL into the free troposphere. Within the boundary layer, vertical mixing is achieved by randomly reassigning the vertical position of the air parcel within the boundary layer, plus a small extra thickness, to allow some parcels to escape the boundary layer, and balance the influx of air parcels from above. This extra thickness, h (in η units), is theoretically derived as (Maryon *et al.* 1991):

$$h = 0.25(2K_\eta\Delta t)^{0.5}. \quad (4)$$

However, using this value caused accumulation of air parcels in the boundary layer, and the value of h was increased by a factor of three to counteract this.

(d) Inter-parcel and convective mixing

The inter-parcel mixing factor (D) was set to a global value of 0.3 in model versions (a) and (b), but reduced to values of 10^{-3} in the η -range 1.0–0.4, and 10^{-6} for η below 0.4, in all other versions. This was to crudely separate mixing in the troposphere and stratosphere.

Mixing between air parcels in regions of convective cloud was introduced in version (d). To represent this sub-grid-scale process, a fraction of the air parcels within a column below the cloud top and above the cloud base are completely mixed. The fraction mixed is related to the vertical mass fluxes within precipitating clouds, and the cloud cover in non-precipitating clouds. In later versions that include convection, convective mixing is extended down to the surface rather than just to the cloud base.

Version (5×5o) was used to tune the convective mixing, by progressively increasing the amount of mixing related to convective cloud cover, until the closest agreement was found with zonal mean July fields from the UM climate resolution run. This tuning was then retrospectively applied in version (e), a version with 10° horizontal resolution. The same tuned scheme was also used in version (5×5c).

(e) *Unified Model version*

The eighth model used was a version of the UK Meteorological Office Unified Model (UM) for climate and weather prediction (Cullen 1993). This is a hydrostatic primitive-equation model; it uses a hybrid (η) vertical coordinate (Simmonds and Burridge 1981), and the Arakawa B grid. A split explicit finite-difference integration scheme is used for the primary model variables (Cullen and Davies 1991). Nineteen vertical levels were used, and the horizontal resolution was 2.5° in latitude and 3.75° in longitude.

Tracers are advected by the model wind field, using a positive definite advection scheme based on a flux redistribution method (Roe 1985). They are also vertically mixed by the model's boundary layer and convection schemes. The strength of the boundary layer mixing depends on the atmospheric stability (see section 2(b) of Smith 1990); the boundary-layer depth varies between one and five model layers accordingly. Convection is parametrized by a penetrative mass-flux scheme (Gregory and Rowntree 1990) in which buoyant parcels are modified by entrainment from and detrainment into the environment. Downdraughts are also represented.

Meteorological data from this model were archived, and used to drive the STOCHEM version (5×5c). As the UM is an established, high resolution GCM, we took the results from this as being our best estimate of reality, in the absence of global coverage of ²²²Rn observations. Some comparisons with the limited observational data set and results from other GCMs are included below.

(f) *Versions used in previous full chemistry experiments*

Existing experiments using the full chemistry version of STOCHEM were performed using some of the above versions of the model transport and mixing. Collins *et al.* (1995) and Stevenson *et al.* (1995) used the same transport scheme as version (b) above. Stevenson *et al.* (1997) used version (d) in a study of aircraft NO_x emissions, and Collins *et al.* (1997), in work on global tropospheric ozone, used a version with high resolution and low values for *D*, but without the NAME BL parametrization, and with untuned convection, a hybrid of versions (b), (c), (d) and (5×5o).

4. RESULTS

(a) *Zonal mean distributions*

Zonal mean distributions of ²²²Rn from the eight models are shown in Fig. 1. These are all June–July–August (JJA) means, except for version (5×5c) which is a July mean. The plots all share some common characteristics: highest values at the surface, particularly in the northern hemisphere, reflecting the source distribution; maximum upward transport is seen in the tropics, even before sub-grid scale convection is added, with a double peak, due to rising air over S.E. Asia (25°N) and Central Africa / S. America (5°N); lowest values are seen in the upper atmosphere of the southern hemisphere, furthest from land sources.

Significant changes are seen between versions (b) and (c), when the mixing factor is reduced, producing a noisier field with less polewards transport, and when the NAME BL

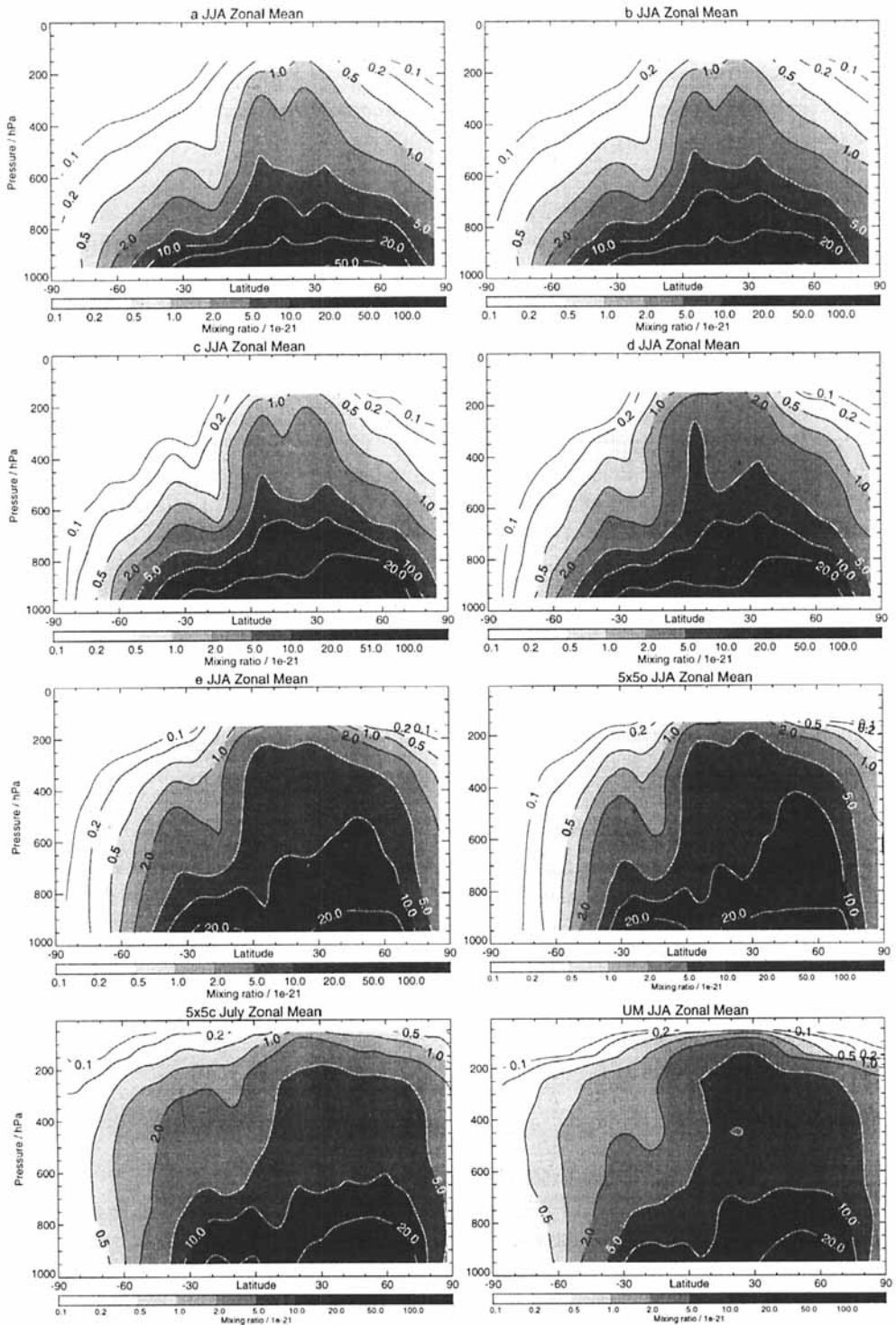


Figure 1. Zonal mean ^{222}Rn fields for the seven versions of STOCHEM (a–e, 5×5o, 5×5c) and the UM. All the plots are for JJA, except 5×5c, which is only for July. The vertical ordinate is $1000 \times \eta$, roughly equivalent to pressure.

mixing and entrainment scheme is added, increasing transport out of the BL and into the free troposphere.

Addition of sub-grid scale convection (version (d)) causes more vertical mixing, particularly in the summer hemisphere tropics, hence reducing surface concentrations and increasing upper tropospheric values. Mixing is only within cloud in version (d), and is achieved by completely mixing a fraction of air parcels within the cloud column (see above).

In version (e) the amount of sub-grid scale convection related to cloud cover was increased, and mixing was extended down to the surface, in order to tune the convection to that seen in the UM. This enhances vertical mixing in the extra-tropics (summer and winter) increases surface transport towards the South Pole, but reduces surface transport towards the North pole.

Increasing the horizontal resolution in version (5×5o) reduces vertical mixing in the tropics slightly, but increases vertical mixing a little in the summer extra-tropics. Polewards transport is reduced, particularly in the southern hemisphere, due to the smaller Eulerian grid boxes used for mixing.

Using six-hourly winds from the climate resolution UM (version (5×5c)), again with a tuned convection scheme produced much more poleward transport, particularly in the southern hemisphere. This version shows excellent agreement with the UM, with tropospheric values always within a factor of two agreement, and generally within 20%. The only obvious discrepancy is at the top of the model, where poor tropopause definition allows transport of too much ^{222}Rn into the stratosphere.

The UM zonal mean shows some ‘mushrooming’, indicative of rapid upward transport of material directly from close to the surface to the upper troposphere. The STOCHEM convective scheme only allows an even redistribution of material below the cloud top. The UM also has a much sharper tropopause, with very little transport of ^{222}Rn into the stratosphere. STOCHEM suffers from its vertically thick layers ($\Delta\eta = 0.1$), over which inter-parcel mixing occurs, making a sharp tropopause difficult to achieve.

Equivalent plots from several global atmospheric transport models that participated in the WCRP 1993 intercomparison are given in Jacob *et al.* (1997). There is generally good agreement between the 3-D models and the UM and versions of STOCHEM that include convection.

(b) Global distributions

Global distributions of ^{222}Rn at the surface, 600 hPa, and 300 hPa, for the eight model versions are given in Figs 2, 3 and 4.

The general characteristics of the surface plots are peak mixing ratios of $50\text{--}100 \times 10^{-21}$ in continental interiors, with values falling below 1×10^{-21} in the central Pacific and over Antarctica. Westerly blown plumes emerge from S. America, S. Africa, and Australasia, at about $40\text{--}50^\circ\text{S}$, and less clear plumes extend from N. America and N. Asia at about $50\text{--}60^\circ\text{N}$. Weaker easterly blown plumes can be seen off the coasts of W. Africa and Central America at about $0\text{--}20^\circ\text{N}$. At 600 hPa, uplift is strongest over tropical America and Africa, and China, with mixing ratios reaching $10\text{--}20 \times 10^{-21}$. These areas are also evident at 300 hPa, with peak values ranging from $5\text{--}20 \times 10^{-21}$, the higher values from versions that include sub-grid scale convection. This process also causes a widespread increase in concentrations over almost the whole upper troposphere, particularly in the summer hemisphere.

The impacts of different boundary-layer schemes can be seen in versions (a), (b), and (c), with a general lowering of peak surface values as first a BL depth is prescribed (b), then BL mixing and upwards entrainment is added (c). Reduction of the mixing factor

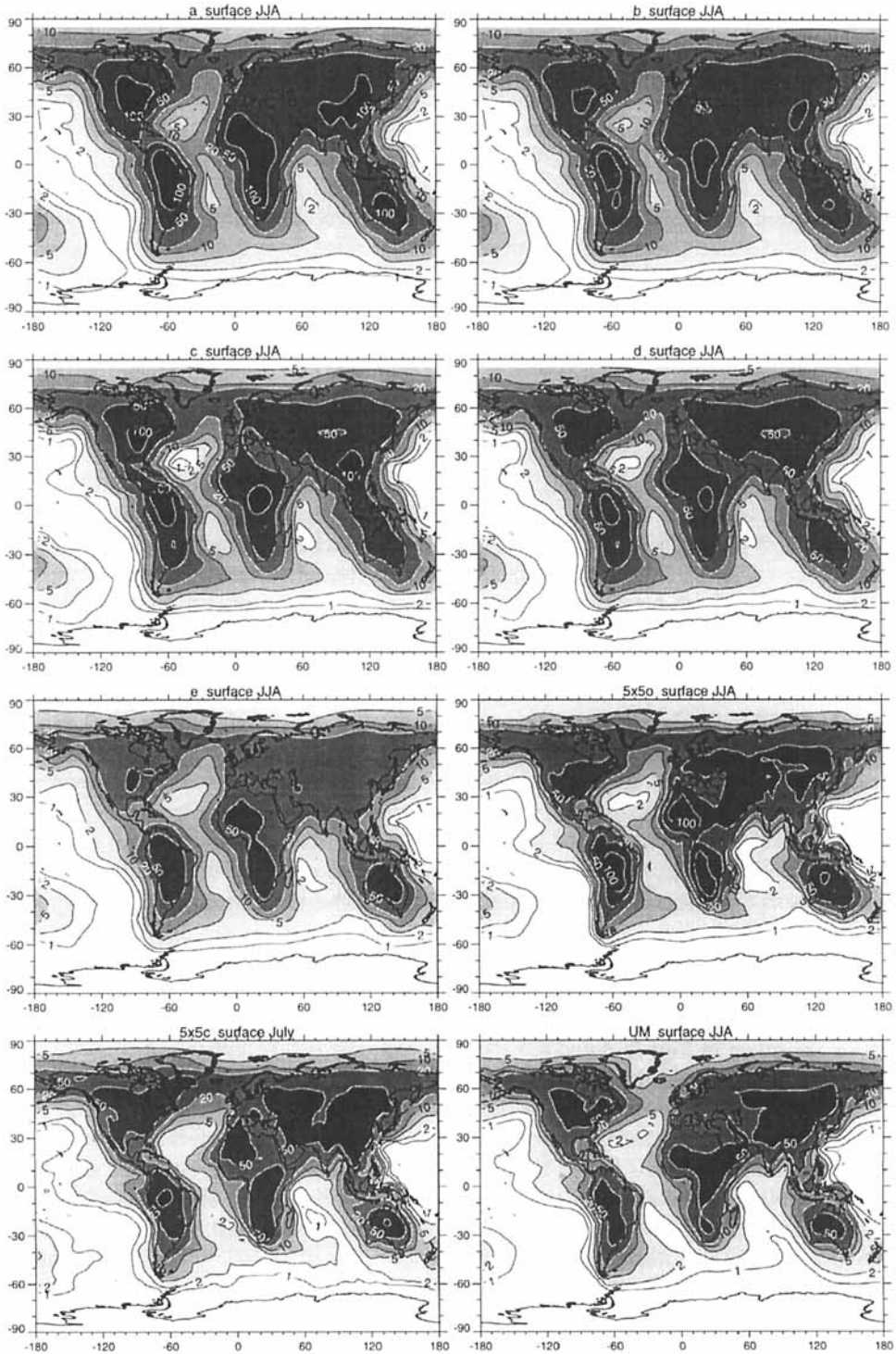


Figure 2. Surface ($\eta = 1.0\text{--}0.9$) ^{222}Rn fields for the seven versions of STOCHEM (a–e, 5×5o, 5×5c) and the UM. The UM field is a weighted mean over the same η range. All the plots are for JJA, except 5×5c, which is only for July.

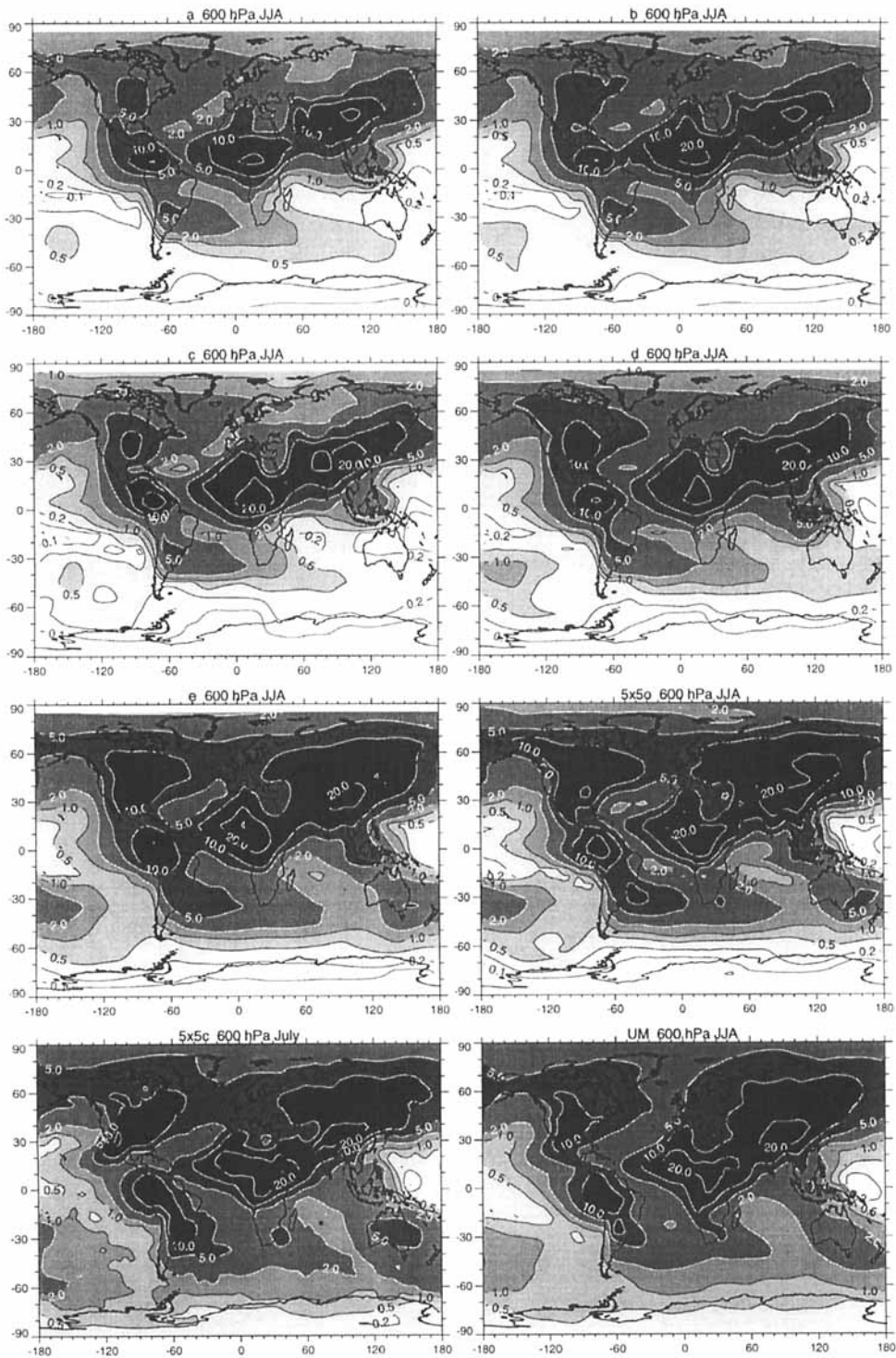


Figure 3. ^{222}Rn fields at approximately 600 hPa ($\eta = 0.5\text{--}0.7$) for the seven versions of STOCHEM (a–e, 5 \times 5e, 5 \times 5c) and the UM. The UM field is for $\eta = 0.60$. All the plots are for JJA, except 5 \times 5c, which is only for July.

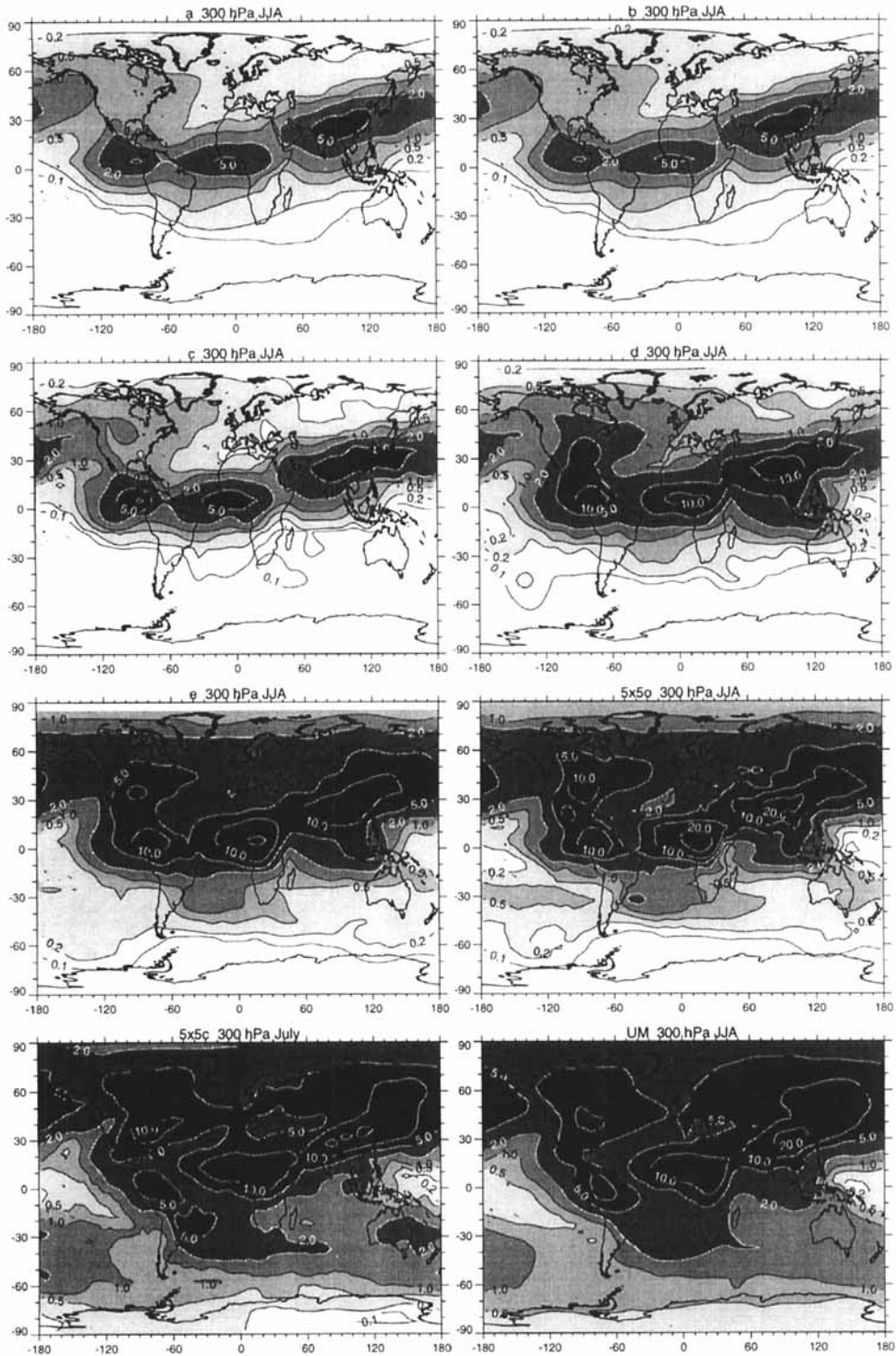


Figure 4. ^{222}Rn fields at approximately 300 hPa ($\eta = 0.2\text{--}0.4$) for the seven versions of STOCHEM (a–e, 5x5o, 5x5c) and the UM. The UM field is for $\eta = 0.30$. All the plots are for JJA, except 5x5c, which is only for July.

produces a more noisy field with tighter gradients (c). Adding sub-grid scale convection (d) reduces summer hemisphere and tropical surface values, transferring material to the upper troposphere. Tuning the convection (e) increases these effects, but also increases surface level transport towards the oceans, and increases winter hemisphere upper tropospheric values. The increase in resolution ($5 \times 5_0$) restores peak surface values to 100×10^{-21} , and tightens coastal gradients. In the upper troposphere, it makes the sites of upwelling more distinct, with slightly higher peaks. Using climate resolution six-hourly winds ($5 \times 5_c$) produces a very similar surface distribution, with marginally more transport towards the oceans. In the mid to upper troposphere, there is more latitudinal transport, and higher values in the summer hemisphere at 300 hPa, but with smaller peaks. Version ($5 \times 5_c$) shows excellent agreement with the UM, the main difference being the smoother fields given by the Eulerian model.

Results for 300 hPa from several other GCMs are reported in Jacob *et al.* (1997). Again, there is good agreement between all of the models that include convection.

5. COMPARISON WITH OBSERVATIONS

Jacob *et al.* (1997) also conducted a comparison of various global transport models with ^{222}Rn observations. Two surface sites (Cincinnati, USA and Crozet Island, Indian Ocean) and two upper troposphere (300 hPa) sites (Hawaii, USA and Kirov, Russia) were chosen, and profiles over northern-hemisphere continents were also used. Model profiles were generated using the mean of results from Kirov, Cincinnati and Socorro (USA). Results from the above runs are presented for JJA in Fig. 5. For each model version the maximum and minimum (upper and lower bars), upper quartile and lower quartile (boxes) and medians (central bar) (mean at Cincinnati) are given, for the whole three month period. Surface results at Cincinnati and Crozet are compiled using mid-afternoon values only, as were the observations. The range of results from the established 3-D GCMs that participated in the model intercomparison of Jacob *et al.* (1997) are also shown in Fig. 5.

Results from the various versions of STOCHEM show remarkably good agreement with the range of values observed at Cincinnati, given that the surface layer has a vertical thickness of about 1 km, a much coarser resolution than most GCMs. Model values for Crozet approach observations as the resolution improves, increasing the number of Eulerian grid boxes between Crozet and S. Africa. Values at both surface stations are reduced when sub-grid scale convection is introduced (d), and variability decreases when the resolution increases. The UM has excellent agreement with observations. Upper atmosphere (300 hPa) model values at Hawaii are all too low; this seems to be a feature of nearly all GCMs (Jacob *et al.* 1997), and may be due an anomalously high ^{222}Rn source in eastern Asia, or possibly a local contribution from the island of Hawaii itself. Values at Kirov fall within the range of observations once the convection scheme has been tuned, and also show a reasonable range.

The impact of convection can also clearly be seen in the profiles over the northern-hemisphere continents in summer (Fig. 6). Profiles are matched closely by versions (e), ($5 \times 5_0$) and ($5 \times 5_c$), whilst the versions (a), (b), and (c), which do not include any sub-grid scale convection, have upper-troposphere concentrations over an order of magnitude too low. The thick horizontal bars on Fig. 6 indicate the range of results reported in Jacob *et al.* (1997) for established 3-D GCMs. The UM tends to produce a C-shaped profile, indicative of rapid upwards transport of in-situ parcels of surface air; this is not seen in the observed profile, and perhaps indicates that the UM convection scheme produces rather too much upwards transport.

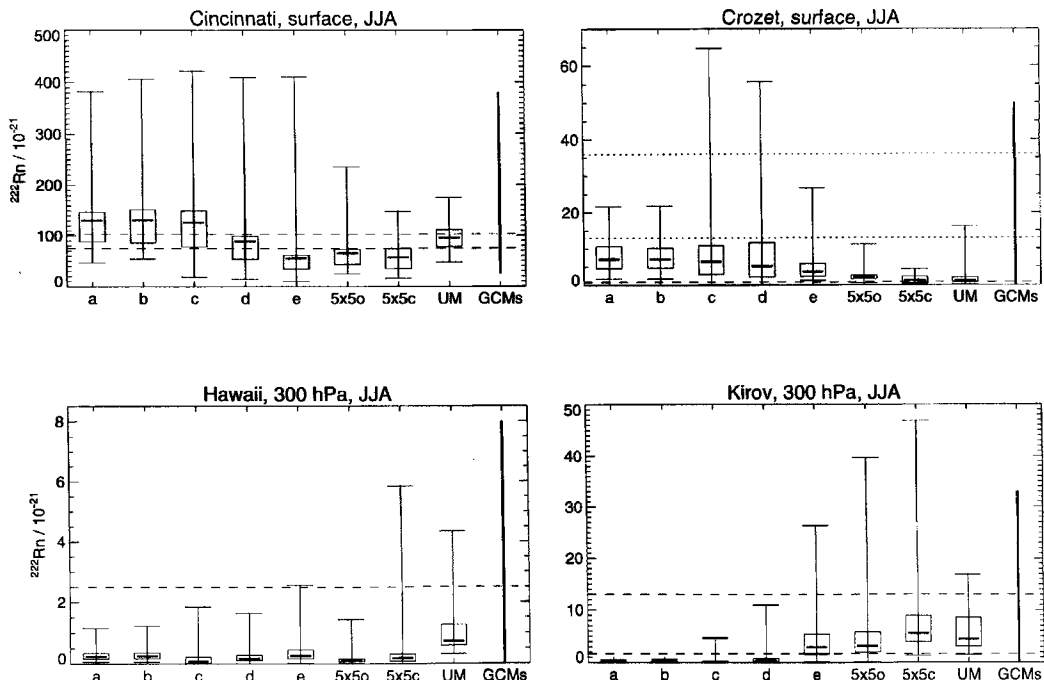


Figure 5. Comparison of modelled and observed values for ^{222}Rn at four locations. Two sites are at the surface (Cincinnati, USA, 40°N , 84°W and Crozet Island, Indian Ocean, 46°S , 51°E), and two are at 300 hPa (Hawaii, USA, 20°N , 155°W and Kirov, Russia, 58°N , 49°E). Results for each model show seasonal extrema (upper and lower bars), upper and lower quartiles (box), and mean (Cincinnati) or median (others) concentration (central thick bar). Cincinnati and Crozet values are calculated using local mid-afternoon values, except for the UM, which uses daily mean values. The dashed lines on the Cincinnati plot show the interannual range of observed mean 1500 LT concentrations, from four years of data, taken from Gold *et al.* (1964). For Crozet, the dashed line is the observed median concentration, and the dotted lines show the interannual range of observed seasonal maxima, taken from 22 years of data (Lambert *et al.* 1995). The dashed line in the Hawaii plot is the observed median of 17 aircraft samples taken at 200 hPa (Kritz *et al.* 1990); the maximum mixing ratio observed was 26×10^{-21} , which is not attained by any model. The dashed lines in the Kirov plot show the range of measured values from four aircraft samples collected over eastern Ukraine in July (Nazarov *et al.* 1970).

6. CONCLUSIONS

Global-scale transport of the short-lived radio-isotope ^{222}Rn has been simulated within a range of UKMO models: several versions of STOCHEM, and the climate resolution version of the UM. This study augments a large model intercomparison and evaluation carried out by the WCRP in December 1993 (Jacob *et al.* 1997). The results illustrate the impact and importance of sub-grid scale convection in vertical redistribution of tropospheric trace gases. Without convection, upper-tropospheric ^{222}Rn concentrations are over an order of magnitude too low, and surface values are about two times too high. The results also show the effect of different boundary layer and mixing schemes, and variations in model spatial and temporal resolutions. Comparisons with observations show improvements as the model resolution increases. Surface stations show reduced variability as resolution increases, whilst upper-tropospheric values show increased variability. STOCHEM transports ^{222}Rn in similar way to the UM and most other GCMs, and results also compare well with the limited observational data set. We conclude that sophisticated Eulerian advection/mixing schemes can be successfully emulated by a computationally inexpensive Lagrangian approach, which is ideally suited to atmospheric chemistry applications.

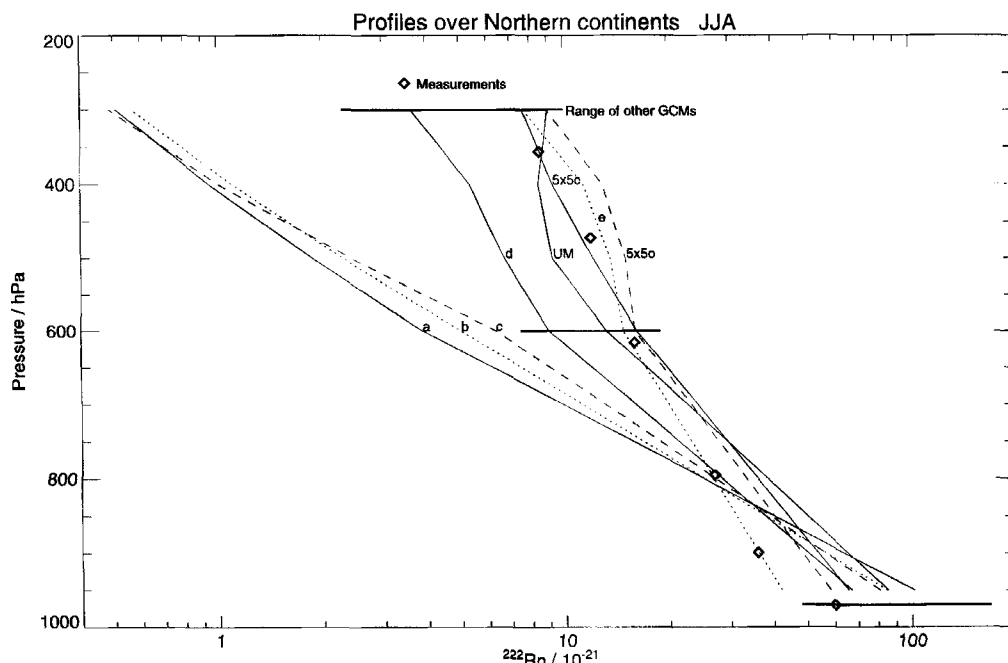


Figure 6. Comparison of modelled and observed vertical profiles of ^{222}Rn over northern continents in summer. Modelled vertical profiles are calculated from the mean of profiles over Cincinnati, Kirov, and Socorro (USA, 34°N , 107°W), using values at approximately 950, 600, 500, 400 and 300 hPa. Each profile is labelled just to its right. The diamonds are observed mean values compiled by Liu *et al.* (1984) from aircraft measurements over North America and Europe. The horizontal bars illustrate the range of values given by established GCMs (models A–J in Jacob *et al.* 1997) that were included in the WCRP intercomparison.

ACKNOWLEDGEMENTS

We wish to thank Roy Maryon, Derrick Ryall and David Thomson for help with parametrizations. David Roberts and Margaret Woodage helped to set up the Unified Model integration. We also thank the UK Department of Environment, Transport, and the Regions, for their help and encouragement through contracts EPG 1/3/17 (Air Quality division) and PECD 7/12/37 (Global Atmosphere division). Comments from two anonymous reviewers helped to clarify and improve the text.

REFERENCES

- | | | |
|---|------|--|
| Atherton, C. S., Penner, J. E., Grotch, S., Parrish, D. D., and Walton, J. J. | 1996 | The role of anthropogenic emissions of NO_x on tropospheric ozone over the North Atlantic: A three-dimensional, global model study. <i>Atmos. Environ.</i> , 30 , 1739–1749 |
| Collins, W. J., Stevenson, D. S., Johnson, C. E., and Derwent, R. G. | 1995 | 'Tropospheric ozone modelled with a global-scale Lagrangian model of diurnal atmospheric chemistry'. Met. Office Turbulence and Diffusion Note No. 224, Atmospheric Processes Research Branch, Meteorological Office, Bracknell, Berkshire, UK |
| | 1997 | Tropospheric ozone in a global-scale three-dimensional Lagrangian model and its response to NO_x emission controls. <i>J. Atmos. Chem.</i> , 26 , 223–274 |
| Cullen, M. J. P. | 1993 | The unified forecast/climate model. <i>Meteorol. Mag.</i> , 122 , 81–94 |
| Cullen, M. J. P., and Davies, T. | 1991 | A conservative split-explicit integration scheme with fourth-order horizontal advection. <i>Q. J. R. Meteorol. Soc.</i> , 117 , 993–1002 |

- Gold, S., Barkhau, H., Shleien, W., and Kahn, B. 1964 'Measurement of naturally occurring radionuclides in air'. Pp. 369–382 in *The Natural Radiation Environment*. Eds. J.A.S. Adams and W.M. Lowder, University of Chicago Press
- Gregory, D., and Rowntree, P. R. 1990 A mass flux convection scheme with representation of cloud ensemble characteristics and stability dependent closure. *Mon. Weather Rev.*, **118**, 1483–1506
- Jacob, D. J., Prather, M. J., Rasch, P. J., Shia, R.-L., Balkanski, Y. J., Beagley, S. R., Bergmann, D. J., Blackshear, W. T., Brown, M., Chiba, M., Chipperfield, M., de Grandpré, J., Dignon, J. E., Feichter, J., Genthon, C. J., Grose, W. L., Kasibahla, P. S., Köhler, I., Kritz, M. A., Law, K., Penner, J. E., Ramonet, M., Reeves, C. E., Rotman, D. A., Stockwell, D. Z., van Velthoven, P. J. M., Verver, G., Wild, O., Yang, H., and Zimmermann, P. 1997 Evaluation and intercomparison of global atmospheric transport models using ^{222}Rn and other short-lived tracers. *J. Geophys. Res.*, **102**, 5953–5970
- Kritz, M. A., Le Rouley, J.-C., and Danielsen, E. F. 1990 The China Clipper. Fast advective transport of radon rich air from the Asian boundary layer to the upper troposphere near California. *Tellus*, **42B**, 46–61
- Lambert, G., Polian, G., Ardouin, B., Renault, J., and Balkanski, Y. 1995 *CFR database of ^{222}Rn , ^{220}Rn , and ^{210}Pb in the sub-Antarctic and Antarctic atmosphere*. Centre des Faibles Radioactivites, Gif-sur-Yvette, France
- Liu, S. C., McAfee, J. R., and Cicerone, R. J. 1984 Radon 222 and tropospheric vertical transport. *J. Geophys. Res.*, **89**, 7291–7297
- Maryon, R. H., Smith, F. B., Conway, B. J., and Goddard, D. M. 1991 The UK Nuclear Accident Model. *Progress in Nuclear Energy*, **26**, No. 2, 85–104
- Nazarov, L. E., Kuzenkov, A. F., Malakhov, S. G., Volokitina, L. A., Gasiyev, Ya. I., and Vasil'yev, A. S. 1970 Radioactive aerosol distribution in the middle and upper troposphere over the USSR in 1963–1968. *J. Geophys. Res.*, **75**, 3575–3588
- Penner, J. E., Atherton, C. S., Dignon, J., Ghan, S. J., Walton, J. J. and Hameed, S. 1991 Tropospheric nitrogen: A three-dimensional study of sources, distributions and deposition. *J. Geophys. Res.*, **96**, 959–990
- Roe, P. L. 1985 Some contributions to the modelling of discontinuous flow. In *Large-scale computations in fluid mechanics*. Eds. B. Engquist, S. Osher, and R. Somerville American Mathematical Society, Providence, Rhode Island
- Simmonds, A. J., and Burridge, D. M. 1981 An energy and angular-momentum conserving vertical finite-difference scheme hybrid vertical coordinates. *Mon. Weather Rev.*, **109**, 758–766
- Smith, R. N. B. 1990 A scheme for predicting layer clouds and their water content in a general circulation model. *Q. J. R. Meteorol. Soc.*, **116**, 435–460
- Stevenson, D. S., Johnson, C. E., Collins, W. J., and Derwent, R. G. 1995 'Changes to tropospheric oxidants from aircraft NO_x emissions studied with a 3-D Lagrangian model.' Met. Office Turbulence and Diffusion Note No. 226, Atmospheric Processes Research Branch, Meteorological Office, Bracknell, Berkshire, UK
- 1997 The impact of aircraft nitrogen oxide emissions on tropospheric ozone studied with a 3-D Lagrangian model including fully diurnal chemistry. *Atmos. Environ.*, **31** 1837–1850
- Taylor, J. A. 1989 A stochastic Lagrangian atmospheric transport model to determine global CO_2 sources and sinks—a preliminary discussion. *Tellus*, **41B**, 272–285
- Thomson, D. J. 1987 Criteria for the selection of stochastic models of particle trajectories in turbulent flows. *J. Fluid Mech.*, **180**, 529–556

- Walton, J. J., MacCracken, M. C. and Ghan, S. J. 1988 A global-scale Lagrangian trace species model of transport, transformation, and removal processes. *J. Geophys. Res.*, **93**, 8339–8354